ACS OMEGA

Open Access

http://pubs.acs.org/journal/acsodf

Article

Reducing the Energy Consumption during Microwave Drying of Coal Slime Dough by Optimizing Parameters: Experiment and Modeling

Fei Wang, Nan Tian, Chen Li, Kai Zhang, Huirong Zhang,* and Yuanyuan Zhang

Cite This: *ACS Omega* 2024, 9, 31986−31997

Read Online

ABSTRACT: Reducing the energy consumption in microwave drying processes is essential for the sustainable management of coal slime. Utilizing a self-constructed microwave thermogravimetric apparatus, the research investigates critical parameters, including microwave power, spherical diameter, and granule size, affecting drying kinetics and energy efficiency. The results show that it was observed that the drying process progresses through three distinct stages, marked by variations in temperature and moisture content: the initial warming phase, a steady drying stage, and a final phase where the drying rate decreases; optimal pellet sizes for efficient moisture evaporation and diffusion were identified, with smaller particles enhancing heat transfer and drying efficiency; and the Nadhari model was determined to best represent the drying kinetics of coal slime under microwave radiation. The findings indicate a positive correlation between drying efficiency and particle size while being inversely related to increased microwave power for smaller granules. A direct positive relationship between moisture migration and increased power levels was established, while an inverse relationship with the enlargement of particle sizes was observed, negatively affecting the efficiency. For granule sizes of 30, 40, and 50 mm, a decrease in activation power was recorded, with values of 8.215 ± 2.301, 7.936 ± 1.547, and 3.393 ± 0.248 $W·g^{-1}$, respectively; and through the comparative analysis of energy consumption, it was demonstrated that for coal slurry particles sized 0.15−0.18 mm subjected to a drying duration of 600 s, an increase in power leads to a reduction in drying efficiency, whereas larger diameter contributes to improved efficiency.

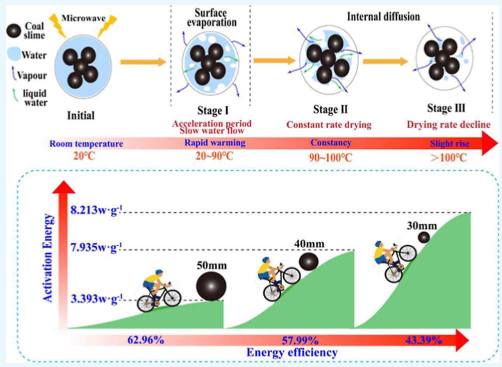

1. INTRODUCTION

Coal slime, a byproduct resulting from the cleaning of unrefined coal, is identified by its high moisture content, substantial viscosity, and reduced calorific value.[1,2] These characteristics significantly impede its further use. It is estimated that by 2025, China will have accumulated over 300 million tons of coal slime. Such an accumulation not only constitutes a considerable waste of resources but also infringes upon land resources and negatively impacts the environment. The processes of dewatering and drying are imperative to increase the energy value of coal slime and to diminish the costs associated with its transportation and storage.[3,4] Therefore, the efficient and low consumption drying of coal slime becomes essential for its reutilization.

Currently, thermal dehydration is acknowledged as the foremost method for extracting moisture from coal slime, involving heat transfer from the exterior to the interior via both convection and conduction, while water is expelled from the interior outward.[5,6] This process, however, can lead to uneven heating and may result in the coal slime's surface hardening, forming a crust. This crusting process obstructs the diffusion of steam, negatively impacts the efficiency of drying, and increases the energy requirements for the drying operation. Moreover, the thermal drying approach depends on gas or superheated steam as the heating medium, which requires a complex heat exchanger of complex design. Such complexity leads to considerable costs in construction and maintenance.[7]

Microwave desiccation technology, which allows materials to absorb microwave radiation and convert it into thermal energy, has garnered considerable interest.[8,9] This technique ensures a more uniform temperature distribution within the material during the heating process. Since the moisture in coal slime exhibits a high dielectric constant and dielectric loss, energy is preferentially directed to the moisture in the coal sludge. Thus, moisture can quickly and efficiently absorb microwave energy and transform it into heat.[10,11] As a consequence, microwave drying markedly improves the efficiency of moisture removal and energy utilization.[12,13]

Received: April 18, 2024
Revised: June 14, 2024
Accepted: June 25, 2024
Published: July 11, 2024

https://doi.org/10.1021/acsomega.4c03638
ACS Omega 2024, 9, 31986−31997

Table 1. Proximate and Ultimate Analysis of Coal Slime

proximate analysis (%)				$Q_{net,ad}$ (J/g)	ultimate analysis (%)				
M_{ar}	A_d	V_d	FC_d*		N_d	C_d	H_d	S_d	O_d
23.08	29.32	26.97	43.71	16,891	0.94	48.99	3.25	1.34	16.16

Table 2. Composition of the Coal Slime (wt %)[a]

SiO_2	Al_2O_3	Fe_2O_3	CaO	MgO	K_2O	Na_2O	P_2O_5	TiO_2
42.19	45.63	4.15	3.13	0.11	0.12	<0.1	<0.1	0.96

[a] M_{ar}, A_d, V_d, FC_d*, and $Q_{net,d}$ represent moisture on received basis, ash on dry basis, volatile matter and fixed carbon, and calorific value, respectively.

In the realm of microwave desiccation, extensive research has been conducted on the drying kinetics of various materials, demonstrating that an optimal combination of microwave radiation intensity and exposure duration significantly enhances the dewatering efficiency of sludge.[14] This approach has also been effective for drying agricultural products, like raspberries, by substantially reducing drying times.[15] Moreover, microwave technology has shown significant promise in the thermal treatment of biomass materials, such as rice husks and sugarcane bagasse, where a microwave power range of 250 to 300 W leads to a noticeable increase in their calorific value.[16] The Midilli−Kucuk model is highly appropriate for describing the thin-layer microwave drying characteristics of lignite across various scenarios, highlighting that both the drying rate constant and the apparent diffusion coefficient increase with the material's diameter and microwave power intensity. This emphasizes the influence of material dimensions and thermal conditions on moisture transfer speed.[17] Further investigations into lignite's microwave drying process indicate that moisture diffusion from the interior toward the exterior is primarily propelled by internal steam pressure, a consequence of uneven moisture evaporation,[17] illustrating the complex multiphase transport mechanism of moisture during drying. For coal slurry, a microwave power of 800 W coupled with a particle diameter of 60 mm has been pinpointed as the optimal drying condition, paving the way for refining the coal slurry drying methodology.[18] The combined use of hot air and microwave drying has been examined as well, revealing how different conditions affect drying rates and their impact on energy consumption, suggesting a nuanced understanding of drying dynamics and efficiency improvements.[18]

Furthermore, the advancement of a complex multiphase porous medium model enables the prediction of moisture transport during microwave heating, revealing that moisture diffusion mechanisms differ between materials with high and low moisture content, attributed to variations in internal pressure gradients. For materials with high moisture content, the elevated internal pressure drives liquid water toward the surface, leading to considerably greater moisture loss in comparison to materials with lower moisture content.[19] However, the exploration of microwave drying for a coal slurry through a spherical model remains relatively uncharted, indicating fertile ground for further investigation.

In this research, a self-made microwave thermogravimetric analyzer was employed to observe the real-time temperature and mass variations in spherical coal dough upon exposure to microwave radiation. The study meticulously examined the influence of microwave radiation intensity, the diameter of the spherical coal dough, and the dimensions of the granules on the drying characteristics of the spherical coal dough. The results of this analysis offer essential knowledge crucial for the design of industrial-scale equipment intended for the drying of coal slime. This contributes significantly to understanding how to optimize drying parameters to improve both the efficiency and effectiveness of coal slime processing.

2. EXPERIMENTAL SECTION

2.1. Raw Materials. Typical coal slime was obtained from the Shuozhou region of Shanxi Province, China, and its basic information is shown in Tables 1 and 2 (XRF). Industrial analysis and elemental analysis were conducted according to the provisions of the national standard, GB212-2022 method, for industrial analysis of coal, with an error margin of 0.3 wt %. The error range of XRF was 5 wt %. Low-temperature ashing of coal slime was conducted at a temperature of 150 °C for obtaining the low-temperature ash (LTA), X-ray diffraction was employed to analyze the mineral composition of coal slime LTA, and the results are presented in Figure 1. The coal slime dough samples with diameters of 30, 40, and 50 mm were prepared by using a spherical mold from coal slime particle size of 0.15−0.18 mm.

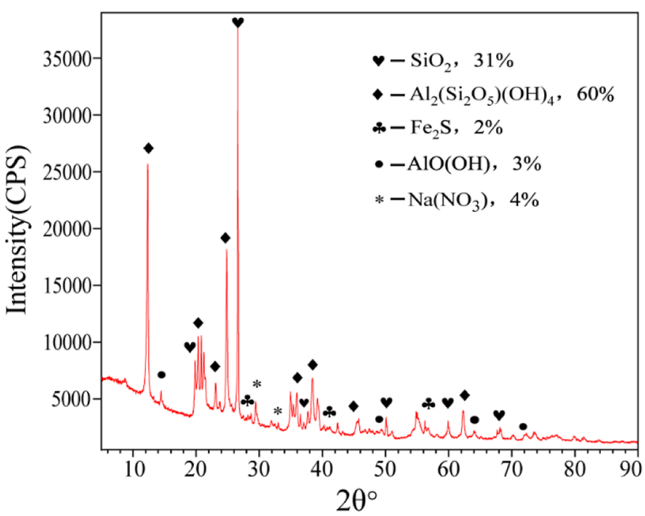

Figure 1. Quantitative mineral composition of coal slime LTA.

2.2. Apparatus and Methods. The experiment was conducted in a self-made microwave workstation with a power of 0−1000 W and frequency of 2450 ± 10 MHz (see Figure 2). The workstation was equipped with a weighing system, which could record the mass and temperature changes in real-time. The experimental procedure for microwave drying of coal slime was as follows: first, a spherical coal slime dough was put into the center of a tray in the microwave workstation.

https://doi.org/10.1021/acsomega.4c03638
ACS Omega 2024, 9, 31986−31997

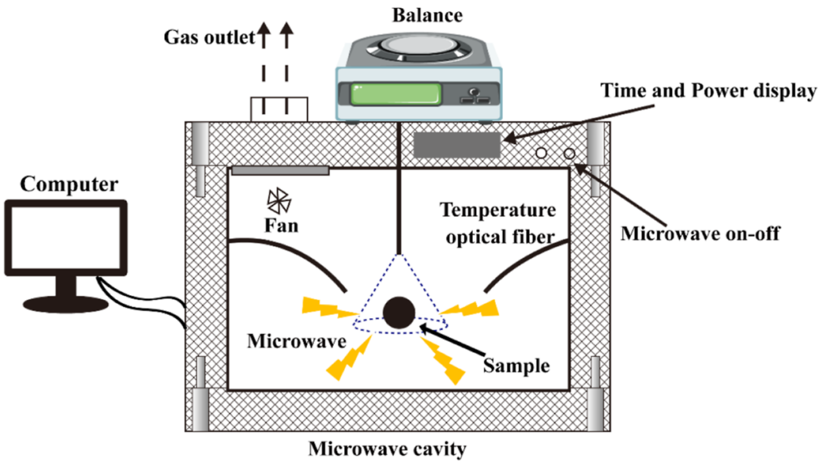

Figure 2. Diagram of the microwave drying experimental setup.

The tray position was fixed at the same position to ensure the repeatability of each measurement. Second, the microwave workstation was started under the selected microwave power, and the microwave drying test was started. The mass and temperature changes during the drying process were recorded by the data acquisition system every 5 s until the end of the test. During the experimental procedure, the error margin for mass was ±0.1 g, and for temperature, it was ±0.1 °C.

2.3. Kinetic Model of Microwave Drying. Material desiccation constitutes a multifaceted process involving coupled heat and mass transfer. The drying kinetic model was of great significance for studying the drying process and predicting the drying process parameters. Key parameters, such as moisture ratio (MR), dry water content, and drying rate, were used to fit the test data. They could be used to describe the drying process of spherical coal slime dough by establishing a suitable kinetic model

$$M_t = \frac{W_t - W_{d,s}}{W_{d,s}} \quad (1)$$

$$\mathrm{MR} = \frac{M_t - M_e}{M_0 - M_e} \quad (2)$$

$$\mathrm{DR} = \frac{M_{t+\Delta t} - M_t}{\Delta t} \quad (3)$$

where M_t is the dry basis water content of the sample at time t; W_t is the total mass of the sample at time t; $W_{d,s}$ is the mass of absolutely dry matter; MR stands for the MR; M_0 refers to the initial water content on a dry basis, i.e., $t = 0$ s; M_e is the equilibrium water content of the sample in the drying experiment;[17] and DR is the drying rate, g water/g dry basis mass s^{-1}, abbreviated as g/g·s^{-1}. Because in microwave drying, it can be assumed that $M_e = 0$,[17] the expression for MR can be written as

$$\mathrm{MR} = \frac{M_t}{M_0} \quad (4)$$

To determine the moisture content trajectory relative to the drying time, the moisture content data obtained from the drying tests was subjected to nonlinear fitting. The most suitable model was found from the six different drying models investigated (Table 3).

Table 3. Drying Mathematical Models

model	equation	constants	references
Page	MR = $\exp(-kt^n)$	k, n	20
Henderson−Pabis	MR = $a\exp(-kt)$	a, k	21
Wang-Singh	MR = $1 + at + bt^2$	a, b	22
Newton	MR = $\exp(-kt)$	k	23
logarithmic	MR =$b\exp(-kt) + a$	a, b, k	24
Nadhari	MR = $a\exp(-kt^n) + b$	a, b, k, n	25

As the main parameters for evaluating the optimal model, the correlation coefficient (R^2), chi-square value (χ^2), residual sum of squares (RSS), and F-value were used to determine the best model from the experimental data. Among these, the closer the correlation coefficient R^2 is to 1, the stronger the correlation; the higher the F-test value, the better the goodness of fit; and the closer the chi-square test χ^2 and the residual sum of squares RSS are to 0, the better the model conforms to the drying law.

3. RESULTS AND DISCUSSION

3.1. Heat Transfer Characteristics at Different Locations within Coal Slurry Spheres. The alterations in moisture phase states within distinct sections of spherical coal slime dough are discernible through temperature variations. In the microwave workstation, optical fibers are employed for real-time temperature monitoring at three specific positions: the center, half the radius, and periphery, throughout the microwave drying of spherical coal slurry agglomerates, as depicted in Figure 3. Consequently, this method enables the identification of each drying stage in the microwave drying process.

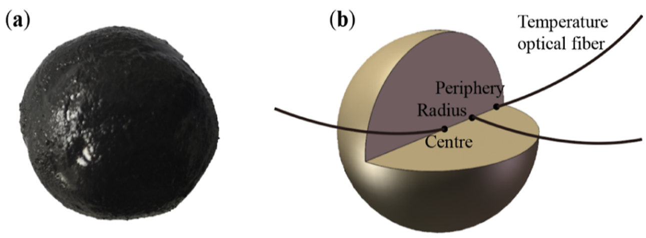

Figure 3. (a) Spherical slime dough and (b) various thermometric points during the test.

https://doi.org/10.1021/acsomega.4c03638
ACS Omega 2024, 9, 31986−31997

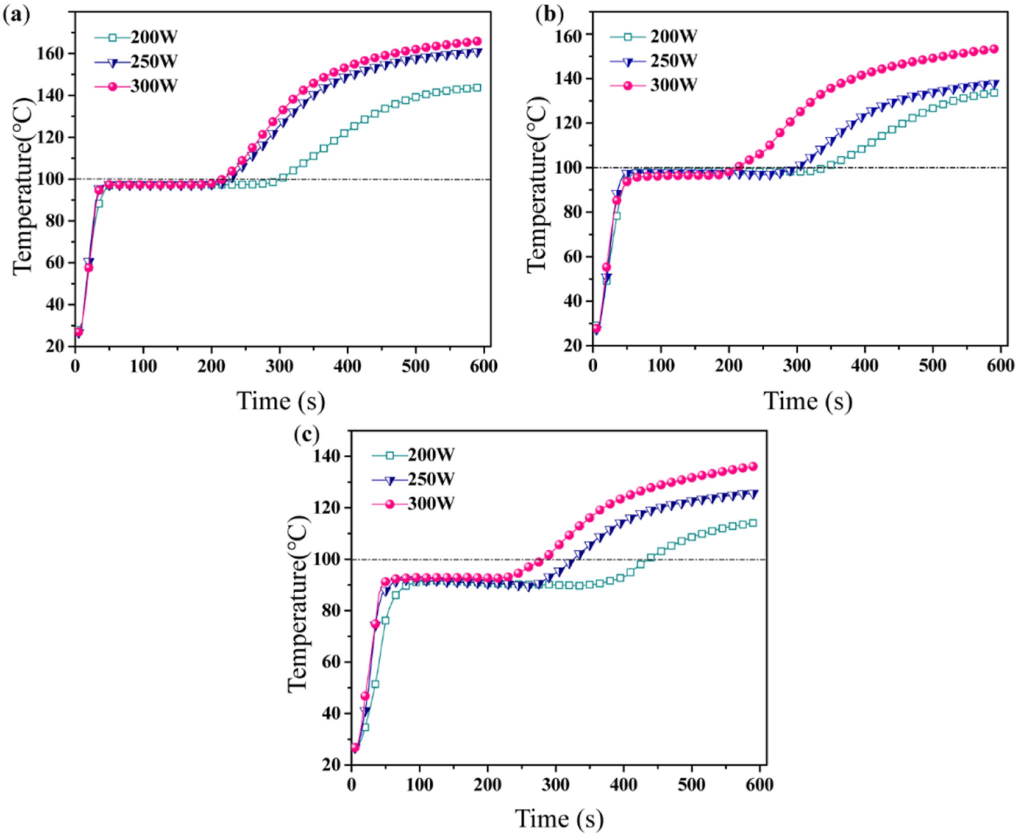

Figure 4. Temperature variations of coal slurry spheres under varying power conditions at the center figure (a), half the radius figure (b), and periphery figure (c).

To explore the temperature distribution of spherical coal slime dough at different powers and to partition different stages in the drying process of spherical coal slime dough, 30 mm spherical coal slime dough samples were selected for microwave drying experiments at 200, 250, and 300 W power, respectively. The temperature distribution during microwave drying can be divided into three stages (Figure 4):

Stage I: the swift preheating phase initiates the drying process, characterized by the high moisture content in spherical coal slime dough. The moisture's loss factor was determined to be 100 times greater than that of carbon, with moisture and dry coal's loss factors being 10 and 0.1, respectively.[18,26] Thus, moisture served as the primary microwave absorber in this phase, rapidly absorbing microwave energy and converting it into heat, resulting in a swift temperature increase in the coal slime dough.

Stage II: the constant temperature stage occurs midway through the drying process, where a significant amount of moisture evaporates. The dynamic equilibrium between heat generated by microwaves and heat absorbed by moisture evaporation is rapidly disrupted, maintaining the temperature inside and on the surface of the spherical coal slime dough at a relatively stable level.[27] The internal equilibrium temperature is slightly below 100 °C, whereas the surface temperature remains lower than the internal temperature due to moisture evaporation predominantly occurring at the surface, a process that absorbs heat and lowers the surface temperature (Figure 4a–c).

Stage III: the secondary reheating stage mainly occurred in the late drying stage. Moisture had been reduced in spherical coal slime dough, and the removal of water was more difficult. The heat absorbed by evaporation is lower than the heat energy contributed by microwave energy, which is absorbed by moisture and dry matter. The temperature in the spherical coal slime dough rose rapidly. During this stage, the microwave energy absorption by the dry components of the coal slime dough becomes increasingly significant.[28]

Additionally, as shown in Figure 4c, it was observed that the time required for the spherical coal slime dough to reach a constant surface temperature decreased from 95 to 70 s with an increase in microwave power. This is attributed to the higher energy absorption per unit volume of coal slime dough at higher power levels, enabling quicker heating to a constant temperature. At the constant temperature stage, the duration of the equilibrium phase shortens as the power increases, reflecting higher efficiency in converting microwave energy into heat. Consequently, the moisture evaporation rate accelerates, leading to reduced water content and a swift transition to the reheating stage. In the final stage, an increase in microwave power corresponds to a higher temperature in the spherical coal slime dough upon completion of the drying process, illustrating the characteristic microwave heating feature where the heat source originates from within the material.

3.2. Mass Transfer and Drying Characteristics in Microwave Drying of Coal Slurry. Microwave drying involves the concurrent interaction of heat and mass transfer phenomena. To understand the complexities of thermo-mass coupling dynamics during the drying process, it is essential to conduct a detailed investigation of coal slurry drying behaviors under different conditions, along with an in-depth analysis of the associated mass transfer mechanisms.

https://doi.org/10.1021/acsomega.4c03638
ACS Omega 2024, 9, 31986−31997

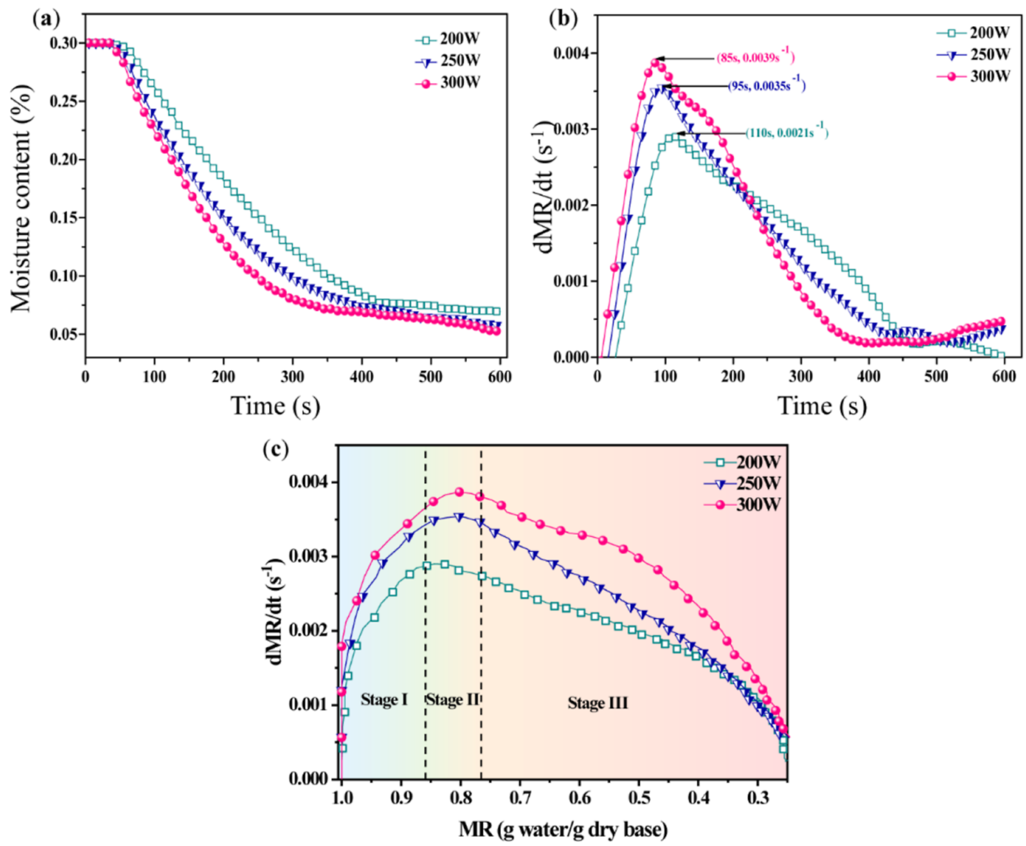

Figure 5. Drying trajectory of spherical coal slime dough subjected to varying conditions: (a) relationship between moisture content and drying time, (b) drying rate varies with drying time, and (c) relationship between drying rate and dry basis moisture content.

3.2.1. Impact of Microwave Power on Drying Characteristics. Microwave power has a great influence on the drying efficiency of the spherical coal slime dough. The drying process of spherical coal slurry with a diameter of 30 mm and particle size of 0.15−0.18 mm was studied under microwave power conditions of 200, 250, and 300 W (Figure 5). Within the desiccation procedure, as depicted in Figure 5b, an escalation in microwave radiation intensity enhanced the desiccation velocity of the spherical coal slime dough, concurrently abbreviating the duration required for drying. The primary cause is attributed to the enhancement of microwave power, which resulted in a heightened volume of microwave absorption per unit volume of the sample. Therefore, the rate of temperature increase in the moisture accelerates at the same time. Concurrently, a microwave of high power is capable of unblocking obstructed pathways, thereby facilitating the enhanced movement of moisture.[29]

When the microwave power is 200, 250, and 300 W, the drying rate of spherical coal slime dough reached 0.0030, 0.0035, and 0.0039 g/g·s^{-1} at 110, 95, and 85 s, respectively. As illustrated in Figure 5b, with the augmentation of microwave power, the time needed for the spherical coal slime dough to achieve its optimal drying rate was reduced. Following the attainment of this peak drying rate, the drying velocity for the spherical coal slime dough began to diminish gradually. The convergence point of the three microwave drying rate curves was noted in the span of 200−250 s, showcasing an identical drying rate at this particular phase. Thereafter, the drying rate of spherical coal slime dough at 300 W was lower than that at the other two powers. The main reason was that spherical coal slime dough at 300 W kept a higher drying rate all the time as drying progressed. Therefore, the loss of moisture from spherical coal slime dough was at most at the same time. The moisture loss of spherical coal slime dough at the other two different power levels during this period was less than that at 300 W. The spherical coal slime dough retained a higher level of residual moisture.

The moisture content at the point of maximum drying rate for spherical coal slime dough exhibited a gradual decrease as the microwave power increased. Taking spherical coal slime dough dried at 300 W as an example, the drying process can be divided into three distinct stages: (1) in the initial stage, spherical coal slime dough under microwave action was rapidly warmed to reach the temperature required for water evaporation. The moisture in the spherical coal slime dough began to decrease slowly during this process. (2) In the second stage, the temperature of the spherical coal slime dough reached a state of equilibrium. The surface water has been removed, and the adsorbed water and part of the capillary water have been evaporated. A steady-rate drying phase occurred as capillary forces replenished the surface-depleted free water (see Figure 4).[18] At this stage, the inner water of the spherical coal slime dough was gradually transformed from a liquid to a gaseous state. The swift accumulation of internal vapor pressure was induced by the vaporization of the liquid water. Moisture in spherical coal slime dough was transferred and diffused from interior to surface under pressure push, that is, the "pumping effect".[30] (3) In the final stage, as the temperature of the coal slurry starts to fall, it heralds the near end of moisture evaporation from the surface of the coal slurry sphere. This period is marked by heightened diffusion resistance to lingering moisture, primarily focusing on the

https://doi.org/10.1021/acsomega.4c03638
ACS Omega 2024, 9, 31986−31997

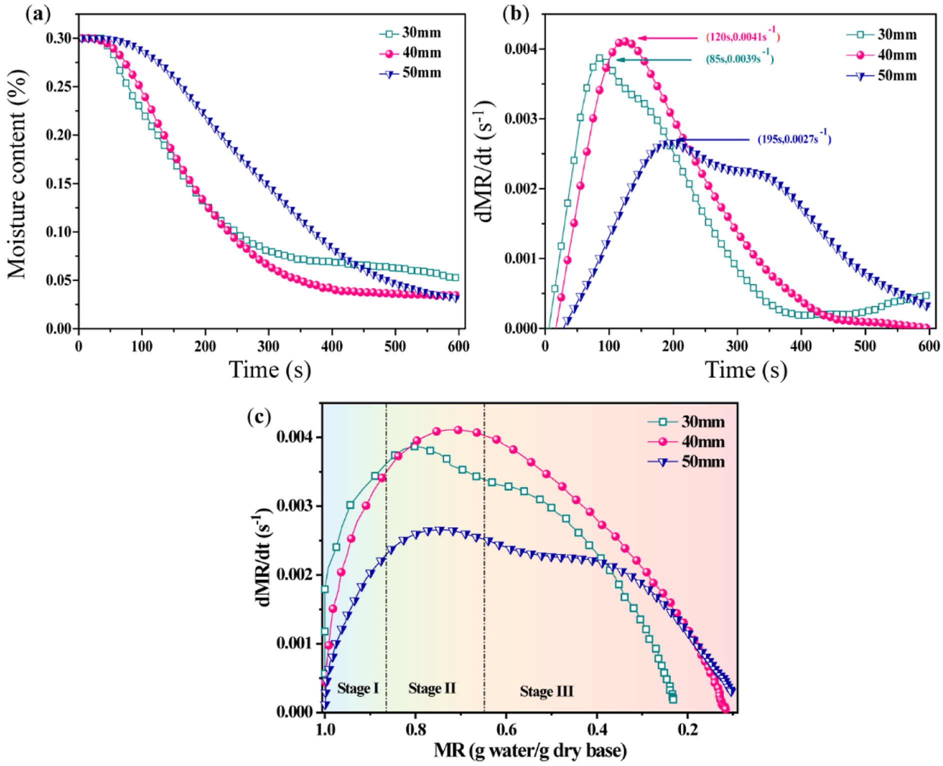

Figure 6. Drying curves of spherical coal slime dough with different diameters. (a) Moisture content changes as a function of drying time; (b) drying rate varies with drying time; and (c) relationship between drying rate and dry basis moisture content.

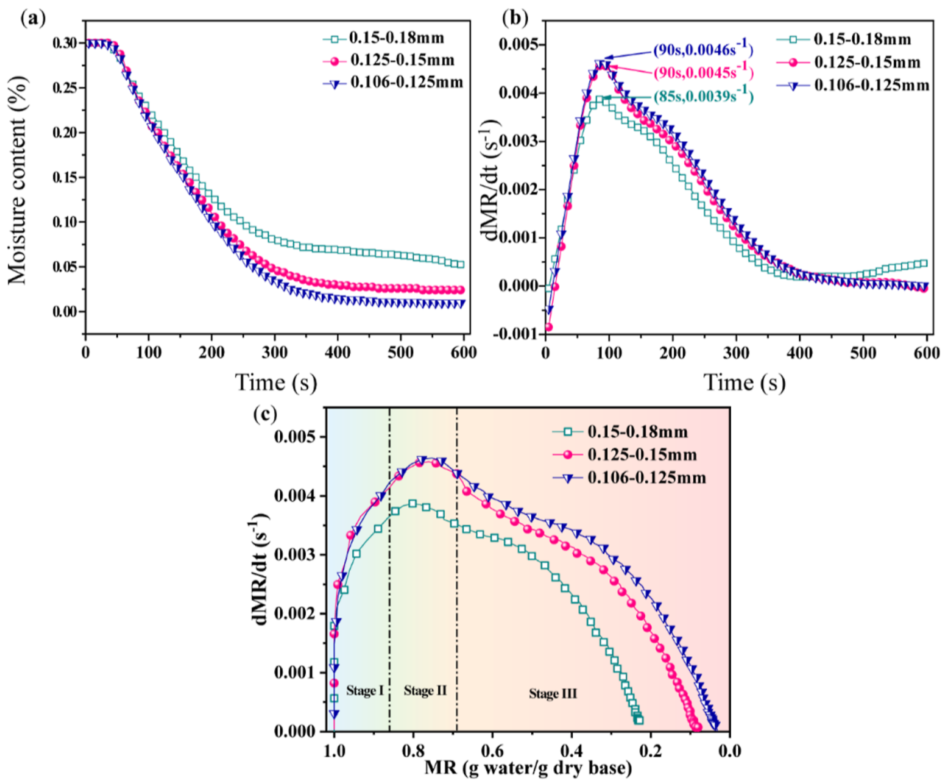

Figure 7. Drying curves of spherical coal slime dough with different particle sizes. (a) Moisture content changes as a function of drying time; (b) drying rate varies with drying time; and (c) relationship between drying rate and dry basis moisture content.

eradication of adsorbed water. Consequently, the removal of moisture at this stage requires overcoming the increased resistance, leading to a gradual decrease in the drying rate.

3.2.2. Influence of Coal Slurry Sphere Diameter on Drying Characteristics. The influence of diameter on the desiccation efficacy of spherical coal slime dough is predominantly

https://doi.org/10.1021/acsomega.4c03638
ACS Omega 2024, 9, 31986−31997

manifested in the extension of the diffusion pathway and moisture concentration. Experiments were conducted on spherical coal slurry dough with diameters of 30, 40, and 50 mm and a particle size range of 0.15−0.18 mm using a drying power of 300 W (Figure 6). Under the same microwave power and coal slime particle size, the drying rate of the spherical coal slurry decreases with the increase in diameter, leading to prolonged drying times. At the start of drying, the 30 mm spherical coal slime shows the highest rate of moisture loss. As time progresses, at 85 s, the 30 mm spherical coal slurry reaches its maximum drying rate, approximately 0.0039 g/g·s^{-1}. At this point, the drying rate of the 40 mm spherical coal slurry is still rising and eventually surpasses that of the 30 mm slime, reaching a peak around 100 s with a drying rate of 0.0041 g/g·s^{-1}. Meanwhile, the 50 mm spherical coal slime takes even longer to reach its maximum drying rate, which is about 0.0027 g/g·s^{-1} at 195 s, as shown in Figure 6b. This phenomenon is ascribed to the initial stage of desiccation, where, given identical moisture levels, the 30 mm spherical coal slime contained the least quantity of water. Moreover, since water is the primary microwave-absorbing substance at the start of drying, it absorbs more energy per unit, as illustrated in Figure 6a, so that equilibrium temperature will be reached more quickly. Therefore, it initially has a higher drying rate. However, as drying progresses, the internal moisture content of the 30 mm slurry decreases, becoming insufficient to absorb all of the released microwave energy. At this stage, the 40 mm spherical coal slurry, having a higher water content than the 30 mm slurry, demonstrates a stronger capacity to absorb microwaves because it has retained more water, leading to an increased drying rate.

3.2.3. Impact of Coal Slime Granule Dimensions on Desiccation Properties. The desiccation characteristics of coal slime are also affected by the size of the coal slime granules. The cross-sectional area for heat dissipation and the dimensions of the water diffusion channels within the spherical coal slime are determined by the particle size. To evaluate the influence of particle size on the drying process, coal slurries with three different particle size ranges were formed into spheres of 30 mm diameter and subjected to a microwave power of 300 W.

The findings indicated that, with constant power and diameter, the drying efficacy of spherical coal slime dough decreased as the particle size of the coal slime increased (Figure 7a), supporting the observations of Yao et al.[30] This suggests that materials with smaller particle sizes exhibit superior drying effects during microwave desiccation.

Further analysis revealed that an increase in granule size led to a corresponding decrease in peak desiccation rates for spherical coal slime dough, with rates recorded as 0.0046, 0.0045, and 0.0039 g/g s^{-1}, respectively. The drying process of coal slime was divided into three stages (Figure 7c), with stage II for slime derived from smaller particle-sized coal being shorter than that for slime with larger particles. The primary reason for this phenomenon is that smaller particle sizes generate stronger capillary forces and form higher water diffusion gradients.[31,32] Additionally, slime spheres made from smaller particles possess a larger specific surface area and more moisture diffusion channels, facilitating easier moisture diffusion and thus exhibiting a higher drying rate.

3.3. Drying Kinetics of Coal Slime and Activation Power. The development of a drying kinetics model offers a more comprehensive insight into the patterns of moisture migration within the spherical coal slurry. By incorporating the various factors outlined in the previous discussions, this model enhances the understanding of the energy transformation and mass transfer dynamics occurring during the microwave desiccation process of a coal slurry. Furthermore, it lays down a theoretical foundation for the engineering and optimization of future desiccation processes specifically designed for spherical coal slurry, enabling more efficient and effective drying strategies.

3.3.1. Drying Kinetic Model. The six drying models were used for the drying experiments. In addition, correlation coefficient (R^2), chi-square (χ^2), RSS, and F value were used to find the best model from the experimental data (Table S1). Meanwhile, the values of the other three parameters also indicate that the Nadhari model is the best model for the microwave drying process of spherical coal slime. This may be due to the increased number of fitting constants in this model compared to other models, as well as the greater length of this model compared to the other models reviewed. The following Table 4 lists all the constants of Nadhari model in the drying process of spherical coal slime.

Table 4. Set of Constants for the Nadhari Model under the Same Drying Conditions

	diameter		
power	30 mm	40 mm	50 mm
200 W	$a = 0.798$	$a = 0.874$	$a = 0.835$
	$b = 0.224$	$b = 0.142$	$b = 0.173$
	$k = 5.534 \times 10^{-5}$	$k = 9.583 \times 10^{-6}$	$k = 4.861 \times 10^{-7}$
	$n = 1.789$	$n = 2.024$	$n = 2.368$
250 W	$a = 0.835$	$a = 0.909$	$a = 0.934$
	$b = 0.203$	$b = 0.118$	$b = 0.078$
	$k = 2.654 \times 10^{-4}$	$k = 2.816 \times 10^{-5}$	$k = 1.986 \times 10^{-6}$
	$n = 1.557$	$n = 1.947$	$n = 2.203$
300 W	$a = 0.829$	$a = 0.906$	$a = 0.927$
	$b = 0.203$	$b = 0.119$	$b = 0.086$
	$k = 1.783 \times 10^{-4}$	$k = 3.828 \times 10^{-5}$	$k = 3.201 \times 10^{-5}$
	$n = 1.677$	$n = 1.928$	$n = 2.188$

Mathematical statistics were used to perform regression analysis of the Nadhari model's constants and experimental parameters (the diameter of the globular slime and microwave power). It was used to show the relationship between the constants in the Nadhari model and experimental parameters during drying.

Mathematical statistics were used to perform calculations based on the relevant equations of the Nadhari model ($MR = a \exp(-kt^n) + b$). The expressions for the calculated parameters a−n are shown in Table 5.

Table 5. Expression of Parameters

parameter	expression	R^2
a	$-0.03 - 0.002P + 0.046D + 1.273 \times 10^{-5}P^2 - 0.001D^2 - 6.334 \times 10^{-7}P^2D + 2.983 \times 10^{-6}PD^2$	0.993
b	$0.435 + 0.008P - 0.035D - 2.26 \times 10^{-5}P^2 + 0.01D^2 + 8.114 \times 10^{-7}P^2D - 3.017 \times 10^{-6}PD^2$	0.993
k	$-0.01 + 8.425 \times 10^{-5}P - 1.487 \times 10^{-7}P^2 - 5.787 \times 10^{-7}D^2 - 2.063 \times 10^{-6}PD + 3.256 \times 10^{-9}P^2D + 4.858 \times 10^{-9}PD^2$	0.974
n	$9.866 - 0.067P - 0.184D + 0.001D^2 + 0.001PD - 2.016 \times 10^{-6}P^2D - 5.048 \times 10^{-6}PD^2$	0.992

https://doi.org/10.1021/acsomega.4c03638
ACS Omega 2024, 9, 31986−31997

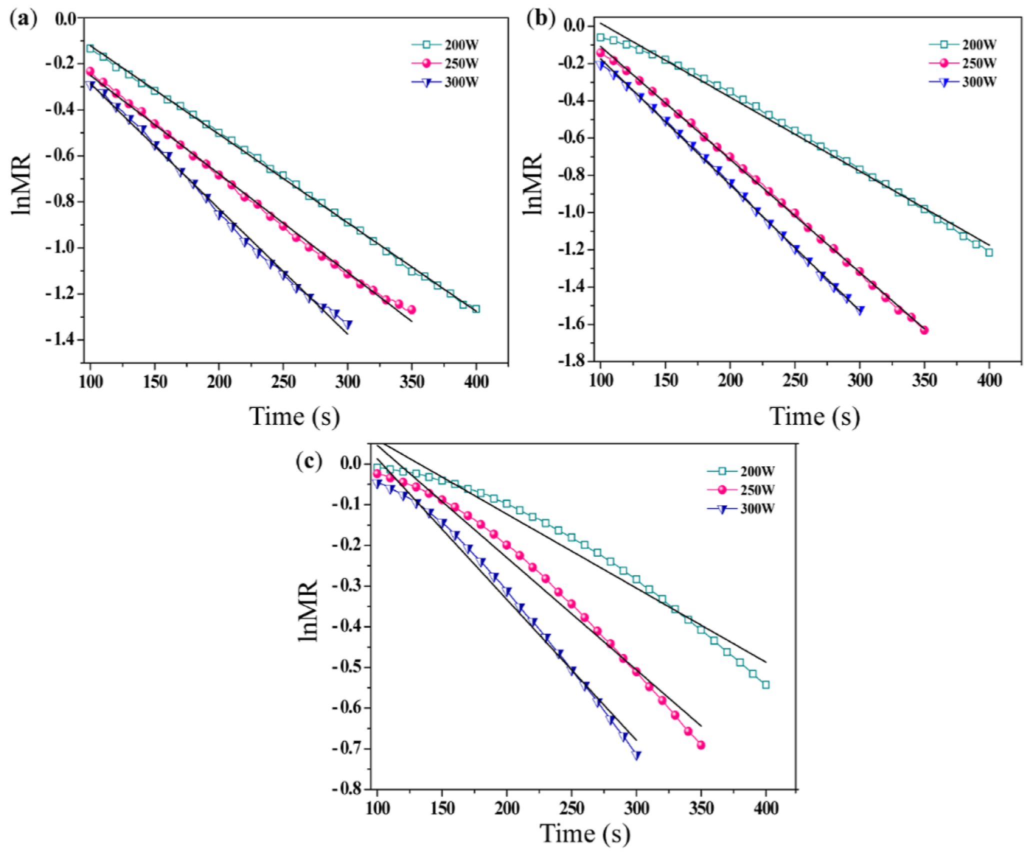

Figure 8. ln MR curves of spherical slime with different diameters under different power as a function of time and (a−c) for spherical slime with diameters of 30 (a), 40 (b), and 50 mm (c).

3.3.2. Effective Diffusion Coefficient and Drying Activation Power. The water in the spherical slurry was removed from the inside to the outside by diffusion. The behavior of spherical coal slurry during drying could be further analyzed by obtaining effective diffusion coefficients under specific conditions by Fick's second law. The foundational assumptions were as follows:[31] the specimen was spherical with initially uniform moisture distribution; external resistance was considered negligible; the effective diffusion coefficient remained constant; and the conditions included constant temperature with minimal shrinkage. Consequently, the equation was formulated

$$\ln\text{MR} = \ln\frac{6}{\pi^2} - \frac{4\pi^2 D_{\text{eff}}}{d^2}t \tag{5}$$

where D_{eff} is effective diffusivity (m^2/s), t is the drying time, d is the sphere diameter (m), and MR is the moisture ratio (kg [H_2O]/kg dry matter). Based on the experimental data, a scatter plot of ln MR versus t can be created. Subsequently, by performing a linear fit, slope k can be obtained. Using this slope k, the effective diffusion coefficient D_{eff} can be determined as follows: $D_{\text{eff}} = \frac{-kd^2}{4\pi^2}$.

In the initial phase of desiccation, the primary impetus for moisture diffusion was the internal vapor pressure. The postulate underlying Fick's second law was found to be inapplicable at this phase.[18] In the last stage of drying, the diffusion of moisture vapor was needed to overcome great resistance. Therefore, the assumption of Fick's second law was not applied at this juncture. With the exclusion of these data to meet the requirements of the linear fit, we chose the data of 100−400 s at 200 W, 100−350 s at 250 W, and 100−300 s at 300 W. The results are shown in Figure 8.

As shown in Figure 9, under the same diameter, the effective moisture diffusion coefficient increases concurrently with the elevation of microwave power. Under the same power conditions, the effective moisture diffusion coefficient increased first and then decreased with the increase in diameter. It is observable that the D_{eff} of 40 mm spherical

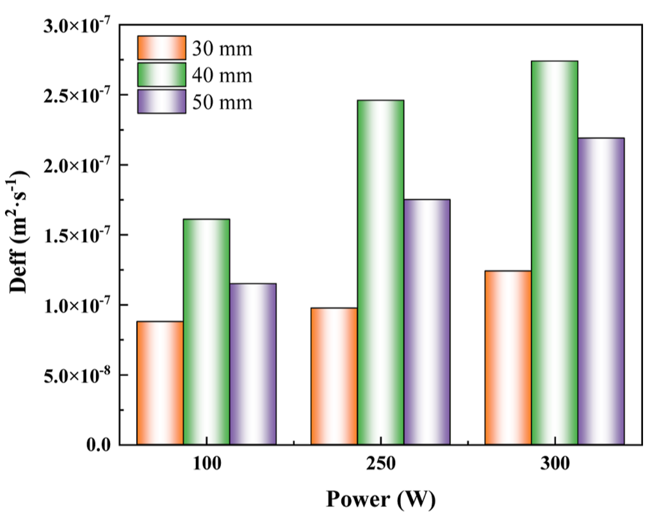

Figure 9. Effective moisture diffusion coefficient of spherical coal slime.

https://doi.org/10.1021/acsomega.4c03638
ACS Omega 2024, 9, 31986−31997

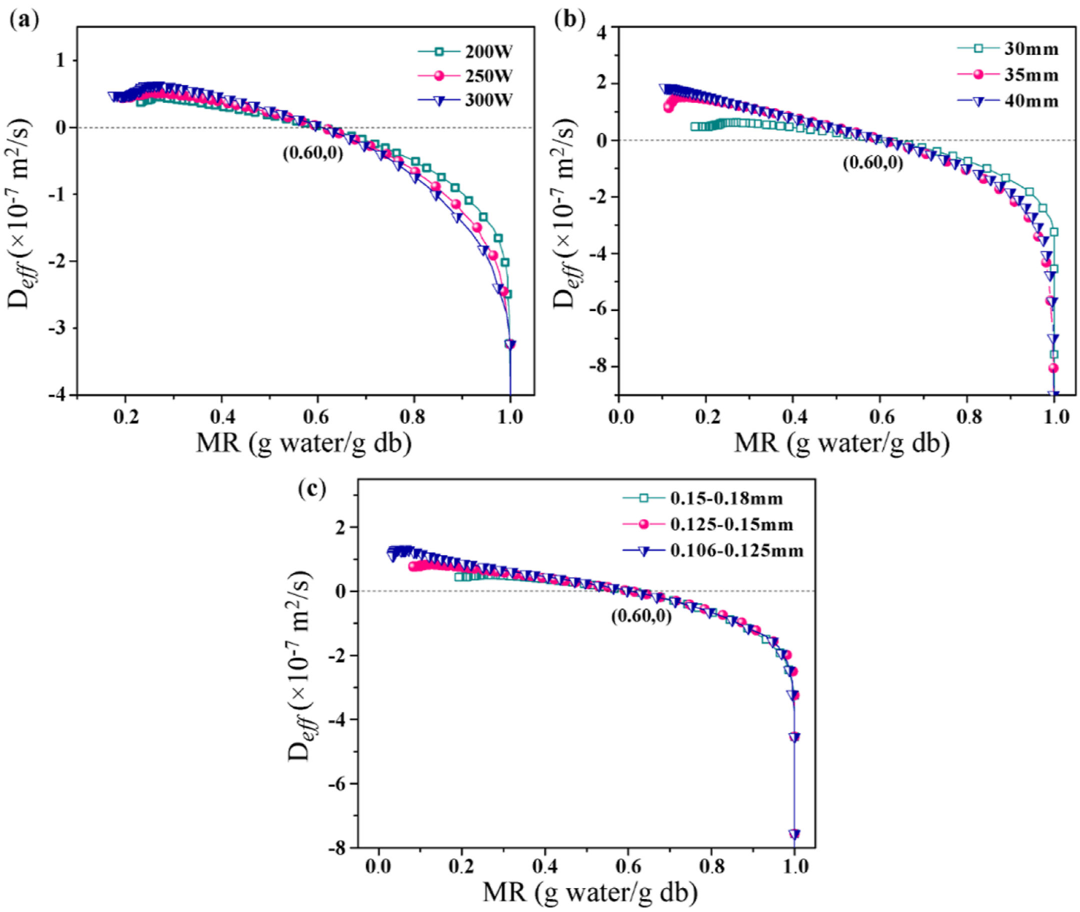

Figure 10. Effective diffusion coefficient of spherical slime under different conditions. (a) Different powers, (b) different diameters, and (c) different particle sizes.

coal slime is the largest at 300 W, reaching 2.74×10^{-7} m^2 s^{-1}. There are two main reasons for this phenomenon: on the one side, an augmentation in diameter results in a heightened internal pressure of water vapor within the specimen, thereby amplifying the evaporation and diffusion of water, which in turn accelerates the drying rate. Conversely, an increase in diameter correlates with an increase in mass, leading to a reduction in the energy absorbed per unit mass when the power level remains constant. At low power levels, the larger diameter of the slurry sample in the microwave field was not fully affected by the action, so the internal moisture temperature of the slurry could not be rapidly increased, while the increase in its moisture diffusion distance also led to increased difficulty of moisture diffusion. Therefore, the effective diffusion coefficient decreased at 50 mm.

Based on the information presented in Figure 8, it was observed that the linear correlation coefficient between the natural logarithm of the MR (ln MR) and time (t) demonstrates a relatively low value. This indicates that the correlation between these variables is not strongly linear over the observed time period. Consequently, the effective diffusion coefficient calculated from this relationship may contain some degree of error. This discrepancy suggests the need for further refinement of the model or the consideration of additional factors that may influence the drying kinetics, such as variable moisture content, uneven heating, or the complex nature of the moisture movement within the spherical coal slurry during microwave drying. Adjusting the model to better reflect these dynamics can enhance the accuracy of the effective diffusion coefficient and provide a more reliable understanding of the drying process.

Building upon the relationship between material moisture content and the effective diffusion coefficient D_{eff}, as proposed by Ruiz Celma,[33] the effective diffusion coefficient D_{eff} can be calculated using the Fourier equation. According to the Fourier equation $F_0 = -4D_{eff}t/d^2$, substituting this into eq 5 and taking the logarithm yields F_0 = −0.05043−0.1013 in MR. Then, substituting $F_0 = F_0 = -4D_{eff}t/d^2$ back into F_0 = −0.05043−0.1013 in MR and rearranging gives

$$D_{eff} = (-0.05043 - 0.1013 \ln MR)d^2/4t \quad (6)$$

Therefore, the relationship image between D_{eff} and MR was obtained.

As illustrated in Figure 10, the effective diffusion coefficient (D_{eff}) of spherical coal slime was observed to increase with the increase in microwave power. This increase in microwave power enhances the energy absorption per unit mass of the spherical coal slurry during the drying phase, consequently accelerating the internal moisture diffusion rate. Thus, an increase in the effective diffusion coefficient occurs. Furthermore, the effective diffusion coefficient exhibits an initial rise followed by a decline as the diameter of the spherical coal slime expands over a specific range and then increases again with a further increase in diameter, suggesting a complex relationship between the diameter of the coal slime and the effective diffusion coefficient.

https://doi.org/10.1021/acsomega.4c03638
ACS Omega 2024, 9, 31986−31997

The variation in particle size also influences the effective diffusion coefficient, with a noted decrease as the particle size of the spherical coal slurry enlarges (Figure 10). Smaller particle sizes contribute to a larger specific surface area of the slurry, allowing for greater energy absorption during the drying process. Additionally, a reduction in particle size is associated with an increased capillary effect, which facilitates the easier diffusion of water.

A consistent phenomenon was observed under three different conditions in the drying process of spherical coal slime: the effective diffusion coefficient approached zero when the MR value was around 0.6. This pattern underscores the nuanced interplay among microwave power, particle size, and structural characteristics of coal slime in determining the efficiency of moisture diffusion during the microwave drying process. It highlights the critical importance of optimizing these parameters to enhance the drying efficiency and effectiveness of coal slime desiccation.

The difficulty of drying the coal slurry under different conditions could be reflected by the magnitude of the activation energy. The activation energy was calculated based on the Arrhenius formula

$$D_{eff} = D_0 \exp\left(-\frac{E_a}{RT}\right) \tag{7}$$

where E_a is the activation power (kJ·mol^{-1}), D_0 is the pre-exponential factor (m^2·s^{-1}), R is the gas constant (8.314 × 10^{-3} kJ·mol^{-1}·K^{-1}), T is the absolute temperature (K), and the values of the effective diffusion coefficient were calculated using Fick's second law, specifically from eq 5. These values correspond to the slopes in Figure 8.

Taking the logarithm of eq 7

$$\ln(D_{eff}) = \ln(D_0) - \frac{E_a}{RT} \tag{8}$$

Making a graph of ln D_{eff} vs $1/T$, with a slope of E_a/R. Given that the microwave drying procedure across varying levels of microwave power did not constitute an isothermal process, the activation power was ascertainable through the adapted Arrhenius equation

$$\ln(D_{eff}) = \ln(D_0) - \frac{E_a m}{P} \tag{9}$$

where m and P are the sample initial mass (g) and microwave power level (W), respectively.

As the diameter of the spherical coal slime increased, but its activation energy decreased continuously. As shown in Figure 11, the activation power of spherical coal slime with diameters of 30, 40, and 50 mm were 8.214 ± 2.301 W·g^{-1}(R^2 = 0.85448), 7.935 ± 1.547 W·g^{-1}(R^2 = 0.9268), and 3.393 ± 0.248 W·g^{-1}(R^2 = 0.98939), respectively. This meant that the larger the diameter of the spherical slurry, the easier it was, in theory, to remove the water. However, considering the actual situation, when the test power is less than or equal to 300 W, the removal effect of 40 mm spherical slime is the highest. This may be because the mass of 50 mm spherical slurry is much larger than that of 40 mm spherical slurry and 30 mm spherical slurry; this results in a lower microwave absorption efficiency per mass and a slower internal moisture warming rate. At the same time, the increase in diameter caused the lengthening of moisture diffusion channels and further increased the resistance to moisture diffusion.

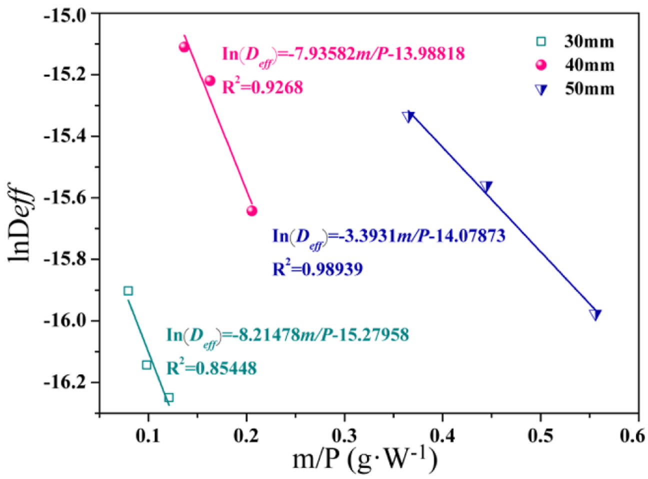

Figure 11. ln D_{eff} under different diameter conditions.

3.4. Energy Consumption Analysis. Energy utilization efficiency holds significant importance when assessing drying technology and is a fundamental requirement for the design and operation of drying equipment. In the context of microwave drying, energy conversion occurs in two distinct stages: the commencement phase entails the transmutation of electrical energy into microwave energy, succeeded by the transformation of microwave energy into beneficial thermal energy assimilated by the material. This process introduces various efficiency considerations. While some analyses have addressed energy utilization, there has been relatively limited exploration of the actual output efficiency in the context of microwave drying. To evaluate the energy consumed in the slime drying process, microwave actual output efficiency was introduced. The efficiency of energy utilization (η) was delineated as the quotient of the energy expended in vaporizing water from the specimen to the total energy consumed, as illustrated in formula 10[18]

$$\eta = \frac{E}{Q} = \frac{\Delta m_t \times \gamma + C_s \times m_t \times \Delta T}{P \times \Delta t \times \theta} \tag{10}$$

where E is the coal slime that absorbs the microwave energy to transform into its own thermal energy; Q is microwave output energy; Δm is the change of slime quality in Δt period; m_t is the slime quality at time t; γ is the latent heat of vaporization of water, 2257.2 kJ/kg; C_s is the specific heat of coal slime, J/(kg·K); ΔT is the change of slime temperature; Δt is the time variation; and θ is the actual microwave output efficiency.

The carbon content in coal slime is significant, exceeding 48%. At room temperature, the loss factor for coal is roughly 0.1, in contrast to that for water, which stands at about 10. This substantial difference indicates that the power absorption capacity of water is approximately 100 times greater than that of coal, implying that water within coal slime should heat more rapidly. This rapid heating of water aids in the microwave drying process, making it an efficient method for removing moisture from coal slime. Given this context, it is reasonable to equate the specific heat (C_s) of coal slime with that of water, estimated at 4.2 × 10^3 J/(kg·°C). This approximation simplifies calculations related to the energy required for heating the mixture of coal and water in coal slime during the drying process. An important consideration in the context of microwave drying is the utilization of waste heat.

https://doi.org/10.1021/acsomega.4c03638
ACS Omega 2024, 9, 31986−31997

To elucidate the nuances of energy consumption efficiency in the microwave drying process of spherical coal slime, particles with a size range of 0.15−0.18 mm were formed into spheres of varying diameters. The energy efficiency of these spherical slimes was then assessed under different microwave power settings over a fixed duration of 600 s (Figure 12). It was observed that an increase in microwave power resulted in a corresponding decrease in the overall energy efficiency of the drying process for the spherical slurry. This decrease in efficiency is linked to the suboptimal utilization of power, where a significant fraction of the increased microwave power did not effectively contribute to the drying of the spherical slurry. Conversely, as the diameter of the spherical slime increased, there was a notable improvement in the overall drying efficiency. This is because a larger diameter results in a greater mass of water in the sludge, which leads to increased microwave absorption. Consequently, the temperature rises more quickly, creating higher internal pressure and thus accelerating moisture diffusion. This improvement can be attributed to the larger diameter of the spherical slime, allowing the microwave power to interact more effectively with the material. Consequently, the energy utilization efficiency of microwaves in the drying process of spherical slime was enhanced. This phenomenon underscores the importance of optimizing both the microwave power settings and the dimensions of the coal slime to be dried, to achieve higher energy efficiency. Such optimizations can lead to more sustainable and cost-effective microwave drying processes, maximizing the efficiency of energy consumption while ensuring thorough drying of the coal slime.

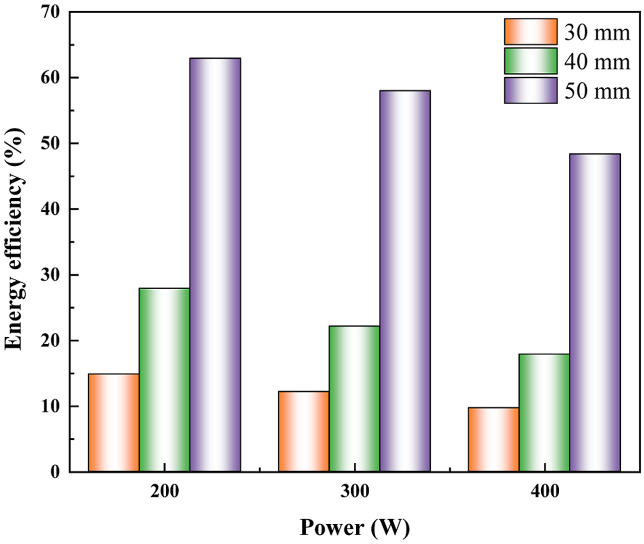

Figure 12. Spherical coal slime drying energy consumption efficiency.

4. CONCLUSIONS

A comprehensive study on the microwave drying characteristics of a spherical coal slurry was conducted using microwave thermogravimetric analysis techniques. The drying kinetics model and drying energy consumption were calculated, yielding the following conclusions:

(1) Based on variations in temperature and moisture levels, the dehydration procedure can be delineated into three distinct stages: the initial warming phase, the period of consistent dehydration rate, and the phase where the dehydration rate decreases.

(2) Optimal pellet diameter for maximum moisture evaporation and diffusion is determined to be 40 mm. A decrease in granule size enhances thermal conductivity, improving the drying process, with an ideal particle diameter between 0.106 and 0.125 mm.

(3) The Nadhari model aptly characterizes the microwave dehydration dynamics of spherical coal slurry. The effective diffusion coefficient of spherical coal slurry increases with both power and particle size but decreases as particle size enlarges. The drying activation power for spherical coal slurry with diameters of 30, 40, and 50 mm are 8.215 ± 2.301, 7.936 ± 1.547, and 3.393 ± 0.248 $W\cdot g^{-1}$, respectively.

(4) Energy efficiency assessments indicate that drying efficiency diminishes with increasing power levels, while larger pellet diameters enhance efficiency. For 50 mm diameter coal slime spheres, the mass results in insufficient microwave absorption per unit volume at 300 W, necessitating an optimal balance of microwave power input and initial material mass for efficient drying.

The findings from this study provide valuable theoretical underpinnings and critical empirical support for the advancement of microwave-enhanced coal slurry drying technology.

■ ASSOCIATED CONTENT

Supporting Information

The Supporting Information is available free of charge at https://pubs.acs.org/doi/10.1021/acsomega.4c03638.

Comparison of experimental parameters of six drying models (PDF)

■ AUTHOR INFORMATION

Corresponding Author

Huirong Zhang − *State Environmental Protection Key Laboratory of Efficient Utilization Technology of Coal Waste Resources, Institute of Resources and Environmental Engineering, Shanxi University, Taiyuan 030006, P. R. China*; orcid.org/0000-0002-7123-749X; Email: zhanghuirong@sxu.edu.cn

Authors

Fei Wang − *State Environmental Protection Key Laboratory of Efficient Utilization Technology of Coal Waste Resources, Institute of Resources and Environmental Engineering, Shanxi University, Taiyuan 030006, P. R. China*; orcid.org/0009-0003-2451-5244

Nan Tian − *State Environmental Protection Key Laboratory of Efficient Utilization Technology of Coal Waste Resources, Institute of Resources and Environmental Engineering, Shanxi University, Taiyuan 030006, P. R. China*

Chen Li − *State Environmental Protection Key Laboratory of Efficient Utilization Technology of Coal Waste Resources, Institute of Resources and Environmental Engineering, Shanxi University, Taiyuan 030006, P. R. China*

Kai Zhang − *State Environmental Protection Key Laboratory of Efficient Utilization Technology of Coal Waste Resources, Institute of Resources and Environmental Engineering, Shanxi University, Taiyuan 030006, P. R. China; Beijing Key Laboratory of Emission Surveillance and Control for Thermal*

Power Generation, North China Electric Power University, Beijing 102206, China

Yuanyuan Zhang − *State Environmental Protection Key Laboratory of Efficient Utilization Technology of Coal Waste Resources, Institute of Resources and Environmental Engineering, Shanxi University, Taiyuan 030006, P. R. China*

Complete contact information is available at: https://pubs.acs.org/10.1021/acsomega.4c03638

Notes

The authors declare no competing financial interest.

■ ACKNOWLEDGMENTS

The work was supported by the Natural Science Foundation of China (22278250) and the Science and Technology Cooperation and Exchange Project of Shanxi Province (202104041101014).

■ REFERENCES

(1) Ning, X.-j.; Liang, W.; Zhang, J.-l.; Wang, G.-w.; Li, Y.-j.; Jiang, C.-h. Effect of ash on coal structure and combustibility. *Int. J. Miner. Metall. Mater.* **2019**, *26*, 973−982.

(2) Zhang, X.; Li, C.; Zheng, S.; Di, Y.; Sun, Z. A review of the synthesis and application of zeolites from coal-based solid wastes. *Int. J. Miner. Metall. Mater.* **2022**, *29*, 1−21.

(3) Li, L.; Jiang, X.; Qin, X.; Yan, K.; Chen, J.; Feng, T.; Wang, F.; Song, Z.; Zhao, X. Experimental study and energy analysis on microwave-assisted lignite drying. *Dry. Technol.* **2019**, *37*, 962−975.

(4) Huang, Y.-F.; Cheng, P.-H.; Chiueh, P.-T.; Lo, S.-L. Leucaena biochar produced by microwave torrefaction: fuel properties and energy efficiency. *Appl. Energy* **2017**, *204*, 1018−1025.

(5) Ling, W.; Xing, Y.; Hong, C.; Zhang, B.; Hu, J.; Zhao, C.; Wang, Y.; Feng, L. Methods, mechanisms, models and tail gas emissions of convective drying in sludge: a review. *Sci. Total Environ.* **2022**, *845*, 157376.

(6) Chen, C.; Venkitasamy, C.; Zhang, W. P.; Khir, R.; Upadhyaya, S.; Pan, Z. L. Effective moisture diffusivity and drying simulation of walnuts under hot air. *Int. J. Heat Mass Transfer* **2020**, *150*, 119283.

(7) Zhao, P.; Liu, C.; Qu, W.; He, Z.; Gao, J.; Jia, L.; Ji, S.; Ruan, R. Effect of temperature and microwave power levels on microwave drying kinetics of Zhaotong lignite. *Processes* **2019**, *7* (2), 74.

(8) Bi, W. B.; Liu, N.; Wang, X. Y. Experimental study on microwave drying characteristics of granite slabs. *Energy Technol.* **2024**, *12*, 2300921.

(9) Mao, S.; Zhou, Y.; Song, B.; Wu, Y.; Wang, Y.; Wang, Y.; Liu, Y.; Xu, X.; Zhao, C.; Liu, J. Effect of microwave intermittent drying on the structural and functional properties of Zein in Corn Kernels. *Foods* **2024**, *13* (2), 207.

(10) Fu, B. A.; Chen, M. Q.; Huang, Y. W.; Luo, H. F. Combined effects of additives and power levels on microwave drying performance of lignite thin layer. *Dry. Technol.* **2017**, *35*, 227−239.

(11) Ge, L.; Liu, X.; Feng, H.; Jiang, H.; Zhou, T.; Chu, H.; Wang, Y.; Xu, C.; Wang, Z. The interaction between microwave and coal: a discussion on the state-of-the-art. *Fuel* **2022**, *314*, 123140.

(12) Yi, L. Y.; Hao, H. W.; Shen, X. S.; Zhang, N.; Huang, Z. C. Drying and roasting characteristics of iron ore pellets with microwave heating. *JOM* **2023**, *75* (9), 3709−3717.

(13) Di, H. K.; Zeng, Y. E.; Song, L. T.; Liang, M.; Hong, Y.; Yang, K.; Zhang, L. B. Microwave drying process and mechanism analysis of viscous germanium-containing residue. *Dry. Technol.* **2023**, *41*, 1803−1814.

(14) Rao, B.; Su, J.; Xu, S.; Pang, H.; Xu, P.; Zhang, Y.; Zhu, J.; Tu, H. Thermal and non-thermal mechanism of microwave irradiation on moisture content reduction of municipal sludge. *Water Res.* **2022**, *226*, 119231.

(15) Gao, Q.; Wang, F.; Wang, J.; Raghavan, V.; Wu, J.; Song, F.; Jin, G.; Song, W.; Song, C. Temperature control for microwave vacuum drying of raspberries. *Dry. Technol.* **2023**, *41*, 2464−2475.

(16) Wang, M. J.; Huang, Y. F.; Chiueh, P. T.; Kuan, W. H.; Lo, S. L. Microwave-induced torrefaction of rice husk and sugarcane residues. *Energy* **2012**, *37* (1), 177−184.

(17) Zhu, J. F.; Liu, J. Z.; Wu, J. H.; Cheng, J.; Zhou, J. H.; Cen, K. F. Thin-layer drying characteristics and modeling of Ximeng lignite under microwave irradiation. *Fuel Process. Technol.* **2015**, *130*, 62−70.

(18) Song, Z. L.; Jing, C. M.; Yao, L. S.; Zhao, X. Q.; Wang, W. L.; Mao, Y. P.; Ma, C. Y. Microwave drying performance of single-particle coal slime and energy consumption analyses. *Fuel Process. Technol.* **2016**, *143*, 69−78.

(19) Ni, H.; Datta, A. K.; Torrance, K. E. Moisture transport in intensive microwave heating of biomaterials: a multiphase porous media model. *Int. J. Heat Mass Transfer* **1999**, *42* (8), 1501−1512.

(20) Zhang, Q.; Litchfield, J. B. An optimization of intermittent corn drying in a laboratory scale thin layer dryer. *Dry. Technol.* **1991**, *9*, 383−395.

(21) Chhinnan, M. S. Evaluation of selected mathematical models for describing thin-layer drying of in-shell pecans. *Trans. ASABE* **1984**, *27*, 610−615.

(22) Wang, G. Y.; Singh, R. P. Single layer drying equation for rough rice. *ASAE Paper No: 78-3001*; ASAE: St. Joseph, MI, 1978.

(23) Ayensu, A. Dehydration of food crops using a solar dryer with convective heat flow. *Sol. Energy* **1997**, *59*, 121−126.

(24) Yagcioglu, A. D.; Cagatay, F. Drying characteristics of laurel leaves under different drying conditions. In *Proceedings of the 7th International Congress on Agricultural Mechanization and Energy in Agriculture, Adana, Turkey*, 1999; pp 565−569.

(25) Nadhari, W. N. A. W.; Hashim, R.; Sulaiman, O.; Jumhuri, N. Drying kinetics of oil palm trunk waste in control atmosphere and open air convection drying. *Int. J. Heat Mass Transfer* **2014**, *68*, 14−20.

(26) Song, Z.; Yao, L.; Jing, C.; Zhao, X.; Wang, W.; Ma, C. Drying behavior of lignite under microwave heating. *Dry. Technol.* **2017**, *35*, 433−443.

(27) Song, Z.; Yao, L.; Jing, C.; Zhao, X.; Wang, W.; Sun, J.; Ma, Y.; Ma, C. Elucidation of the pumping effect during microwave drying of lignite. *Ind. Eng. Chem. Res.* **2016**, *55*, 3167−3176.

(28) Li, L.; Jiang, X.; Bian, Z.; Wang, J.; Wang, F.; Song, Z.; Zhao, X.; Ma, C. Microwave drying performance of lignite with the assistance of biomass-derived char. *Dry. Technol.* **2019**, *37*, 173−185.

(29) Li, H.; Lin, B.; Hong, Y.-d.; Liu, T.; Huang, Z.; Wang, R.; Wang, Z. Assessing the moisture migration during microwave drying of coal using low-field nuclear magnetic resonance. *Dry. Technol.* **2018**, *36*, 567−577.

(30) Yao, L.; Song, Z.; Sun, C.; Zhao, X.; Wang, W.; Mao, Y.; Sun, J.; Wang, T. Study on the evolution of internal and external water of lignite during microwave drying and the moisture reabsorption characteristics of dried lignite. *Energy Sources, Part A Recovery, Util. Environ. Eff.* **2020**, *42*, 1−18.

(31) Ratanadecho, P.; Aoki, K.; Akahori, M. Experimental and numerical study of microwave drying in unsaturated porous material. *Int. Commun. Heat Mass Transfer* **2001**, *28*, 605−616.

(32) Ratanadecho, P.; Aoki, K.; Akahori, M. Influence of irradiation time, particle sizes, and initial moisture content during microwave drying of multi-layered capillary porous materials. *J. Heat Transfer* **2002**, *124*, 151−161.

(33) Celma, A. R.; Cuadros, F.; López-Rodríguez, F. Convective drying characteristics of sludge from treatment plants in tomato processing industries. *Food Bioprod. Process.* **2012**, *90* (2), 224−234.

https://doi.org/10.1021/acsomega.4c03638
ACS Omega 2024, 9, 31986−31997